TB, RM, CQG/197635, 4/08/2005

INSTITUTE OF PHYSICS PUBLISHING CLASSICAL AND QUANTUM GRAVITY

Class. Quantum Grav. **22** (2005) 1–11 doi:10.1088/0264-9381/22/0/000

The AURIGA–LIGO joint burst search

L Cadonati[1], L Baggio[2,9], I S Heng[3], W Johnson[4], A Mion[2], A Ortolan[5], S Poggi[2], G A Prodi[2], F Salemi[6], P Sutton[7], G Vedovato[8], M Zanolin[1] and J P Zendri[8]

[1] Massachusetts Institute of Technology, LIGO Laboratory, NW17-161 Cambridge, MA 02139, USA
[2] Physics Department, University of Trento and INFN, via Sommarive 14, I-38050 Povo (Trento), Italy
[3] Department of Physics & Astronomy, University of Glasgow, Glasgow, G12 8QQ, UK
[4] Physics Department, Louisiana State University, Baton Rouge, LA, USA
[5] Laboratori Nazionali di Legnaro, INFN, viale dell'Università 2, I-35020 Legnaro (Padova), Italy
[6] Physics Department, University of Ferrara and INFN Laboratori Nazionali di Legnaro, viale dell'Universitá 2, I-35020 Legnaro (Padova), Italy
[7] LIGO Laboratory, California Institute of Technology, Pasadena, CA 91125, USA
[8] INFN Sezione di Padova, via Marzolo 8, I-35131 Padova, Italy

E-mail: cadonati@ligo.mit.edu

Received 1 April 2005, in final form 26 July 2005
Published DD MMM 2005
Online at stacks.iop.org/CQG/22/1

Abstract
Over the course of a 2-week period, starting on Christmas Eve 2003, the recently upgraded AURIGA and the LIGO observatory were simultaneously acquiring data. This first coincidence run between the two projects triggered a new collaborative effort in the search for gravitational wave bursts. This paper introduces the goals of the AURIGA–LIGO joint analysis and the methods that have been formulated to address the challenges of a coincidence between detectors with different spectral sensitivities, bandwidths and antenna patterns. Two approaches are presented, both based on the exchange of event triggers between AURIGA and LIGO: a set of directional coincidence searches, which exploit measured amplitude information, and a cross-correlation search in the LIGO interferometers around the time of the AURIGA events, with minimal assumptions on the signal characteristics.

PACS numbers: 95.55.Ym, 04.80.Nm, 07.05.Kf

(Some figures in this article are in colour only in the electronic version)

[9] Currently at Institute for Cosmic Ray Research, University of Tokyo, 5-1-5 Kashiwanoha, Kashiwa, Chiba, 277-8582, Japan.

1. Introduction

Over the course of a 2-week period, starting on Christmas Eve 2003, the recently upgraded AURIGA resonant bar detector and the Laser Interferometer Gravitational Wave Observatory (LIGO) were simultaneously acquiring data. This was the first coincident run between the two projects and an important opportunity for a collaborative analysis. In July 2004, the two projects signed a Memorandum of Understanding [1] for a coincident burst search between LIGO and AURIGA, to be performed on data acquired between 24 December 2003 and 9 January 2004. This data set is part of the third LIGO Science Run (S3) and the first run of the upgraded AURIGA detector (AU1). It includes 92 h of quadruple coincidence between AURIGA and the three LIGO interferometers and 175 h of triple coincidence between AURIGA and two LIGO interferometers. Due to the short duration of the S3/AU1 coincident observation, the results of this analysis are not expected to have an impact comparable to that of longer data-taking runs [2, 3]. Nevertheless, this effort is important as a methodological study laying the path for future, longer coincidence runs between detectors with very different spectral sensitivities.

In order for the network to achieve its potential, all the detectors should have comparable sensitivity to the target signals. In this case, the addition of a resonant bar (AURIGA) to a network of long-baseline interferometers (the LIGO observatory) can provide significant benefits only for signals with a detectable spectral component in the bar's narrower sensitivity band. Therefore, the AURIGA–LIGO joint search focuses on bursts with high-frequency content, such as black hole ring downs [4] and mergers of coalescing neutron star or black hole binary systems [5].

The initial plan is to perform a trigger-based coincidence search, following the methods described in section 5. The exploration of coherent analysis techniques for burst searches is also being considered as the focus of a possible second round of studies.

The paper is organized as follows: section 2 offers an overview of the detectors' performance during the analysis period; section 3 discusses antenna patterns and sky coverage; section 4 lists the scientific motivations for the joint analysis and section 5 presents the methods explored by the joint analysis team, with a preview of the expected performance.

2. Performance of the network in the coincidence run

The AURIGA detector has been upgraded since its original run (1997–1999) [6]. The principal improvements have been achieved on the signal amplifier and signal matching network, on the cryogenic suspensions and on the data analysis system [7]. The initial phase of the upgraded AURIGA run was carried out at liquid helium temperatures (4.5 K during the overlapping period with LIGO S3). The higher operating temperature caused the minima of the noise power spectrum S_{hh} to be higher than during the original run, when the operating temperature was 0.2 K. Nevertheless, the sensitivity to transient signals has improved, thanks to the significant enlargement of the sensitivity band. The spectral sensitivity is much flatter, with a FWHM bandwidth of 30 Hz, and the energy sensitivity to millisecond transients is about three times better than the best performance achieved during the original run. The AU1 run was the first continuous period of data acquisition in the target configuration for the upgraded AURIGA. It started on 24 December 2003 and ended on 13 January 2004.

The third LIGO Science Run (S3) covered a 10-week period between 31 October 2003 and 9 January 2004. The fundamental improvement from the previous S2 run is a reduction on H1–H2 correlated noise, thanks to the suppression of acoustic coupling. H1 offers the best spectral improvement since S2, although it presents an increased rate of transient glitches.

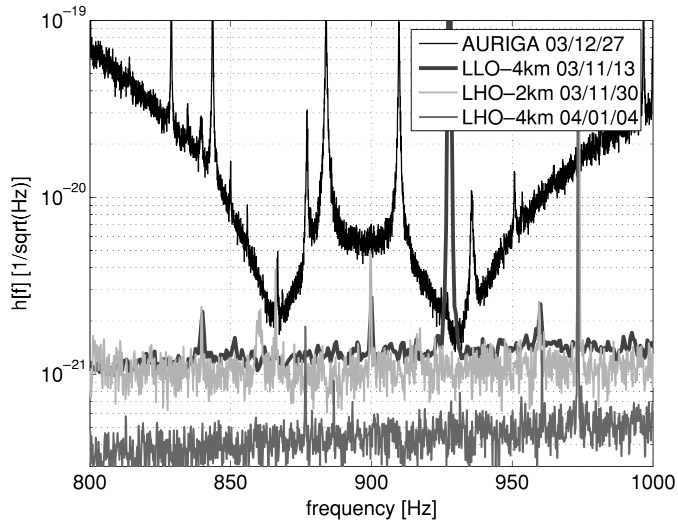

Figure 1. Single-sided sensitivity spectra for AURIGA and the three LIGO interferometers during the AU1 and S3 science runs in the 800–1000 Hz band. Note, in the AURIGA spectrum, the presence of spurious lines. For LIGO, the Hanford spectra are quite representative, but the Livingston spectra were at times a factor 2–3 worse than shown here (on this topic, see also figure 2). In the LIGO spectra, also note the calibration lines at 973 Hz for the Hanford detectors and 927 Hz for the Livingston detector, inconveniently centred in one of the two AURIGA minima. AURIGA's spurious lines and LIGO's calibration lines need to be filtered in the analysis.

L1 was arguably the most problematic of the three interferometers, as it had the lowest duty cycle and the largest variability in spectral shape: the noise floor in the band of interest for this analysis fluctuated by up to a factor 3 over the course of the run.

Figure 1 shows the best single-sided sensitivity spectra in the 800–1000 Hz band for AURIGA and the three LIGO interferometers during the AU1 and S3 runs. The AURIGA spectrum features several spurious lines, whose amplitude is non-stationary and affected by human activities. These lines do not appear in the mechanical or electromagnetic transfer functions but are generated by up-conversion of low-frequency noise. The AURIGA data analysis had to be modified to take them into account, with an adaptive algorithm that tracks the variation of the spurious lines and partially whitens the spectrum. When the non-stationarity is too rapid for the algorithm, the spurious lines are notched by narrow Butterworth band-reject filters.

The LIGO spectra are quite flat in the analysis band; the dominant features are the calibration lines at 973 Hz for the Hanford detectors and 927 Hz for the Livingston detector, inconveniently centred in one of the two AURIGA minima.

Figure 2 shows the root-sum-square amplitude required for a test waveform to have signal-to-noise ratio $\rho = 1$ in each detector over the analysis period. The test waveform is a sine-Gaussian of the form

$$h(t) = h_0 \sin[2\pi f_0 (t - t_0)]\, \mathrm{e}^{-\frac{(t-t_0)^2}{\tau^2}}, \tag{1}$$

with central frequency $f_0 = 900$ Hz and $\tau = 2/f_0$, corresponding to quality factor $Q = \sqrt{2}\pi\tau f_0 = 8.9$. The signal-to-noise ratio ρ is defined, according to [4], as

$$\rho = \left[4 \int_0^\infty \mathrm{d}f \frac{|\tilde{h}(f)|^2}{S(f)} \right]^{1/2}, \tag{2}$$

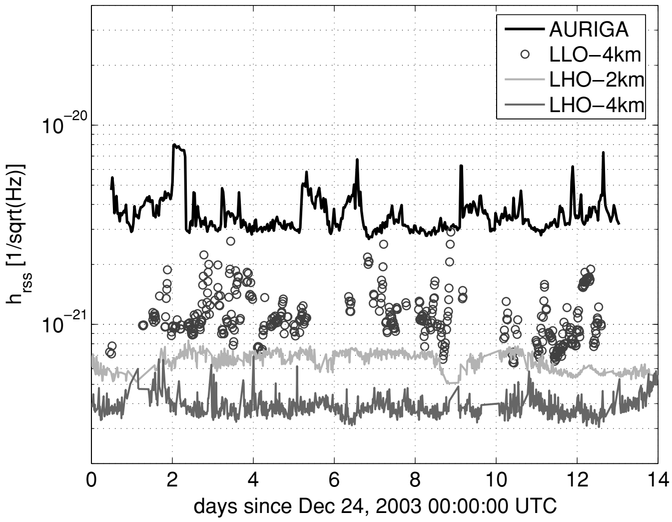

Figure 2. Root-sum-square amplitude h_{rss} of a 900 Hz sine-Gaussian with $Q = 8.9$ with SNR = 1 in AURIGA and in the LIGO interferometers over the period of interest for this analysis. The sine-Gaussian waveform, root-sum-square amplitude and SNR are defined in equations (1)–(3).

where $S(f)$ is the single-sided detector noise. The root-sum-square amplitude h_{rss} is defined as

$$h_{\mathrm{rss}} = \left[\int_{-\infty}^{\infty} \mathrm{d}t |h(t)|^2\right]^{1/2} = \left[2\int_{0}^{\infty} \mathrm{d}f |\tilde{h}(f)|^2\right]^{1/2}. \tag{3}$$

The data in figure 2 is obtained analytically from the noise spectrum. Equation (2) is solved for $\rho = 1$ and the resulting h_0, function of time, is used to compute the corresponding h_{rss} from equation (3). The actual amplitude or SNR at which a signal is detectable with a specified efficiency depends on the details of the search algorithm, on the non-gaussianity of the data and on the thresholding scheme, which in turn is regulated by the false alarm rate and by the allowed bias on the estimated event parameters (amplitude and arrival time).

3. Antenna patterns and sky coverage

An important factor in evaluating the efficiency of a network is the sky coverage, which depends on the antenna pattern of all participating detectors.

The antenna pattern F_i describes the radiation pattern of the ith detector with respect to its geometry and position. In its most general form, it can be expressed as

$$F_i(\theta, \phi, \psi) = A_i(\theta, \phi)\cos[2\psi + \delta(\theta, \phi)], \tag{4}$$

where θ and ϕ are the declination and right ascension angles describing the source position in the sky, ψ is the polarization angle of the incoming gravitational wave, δ is a phase shift and the magnitude is $A_i = \sqrt{F_{i+}^2 + F_{i\times}^2}$.

The antenna pattern magnitudes for the AURIGA and LIGO-Hanford (LHO) detectors are shown in figure 3. Their combined directional sensitivity can be expressed through the product

$$F_1F_2 = \tfrac{1}{2}A_1A_2[\cos(4\psi + \delta_1 + \delta_2) + \cos(\delta_1 - \delta_2)]. \tag{5}$$

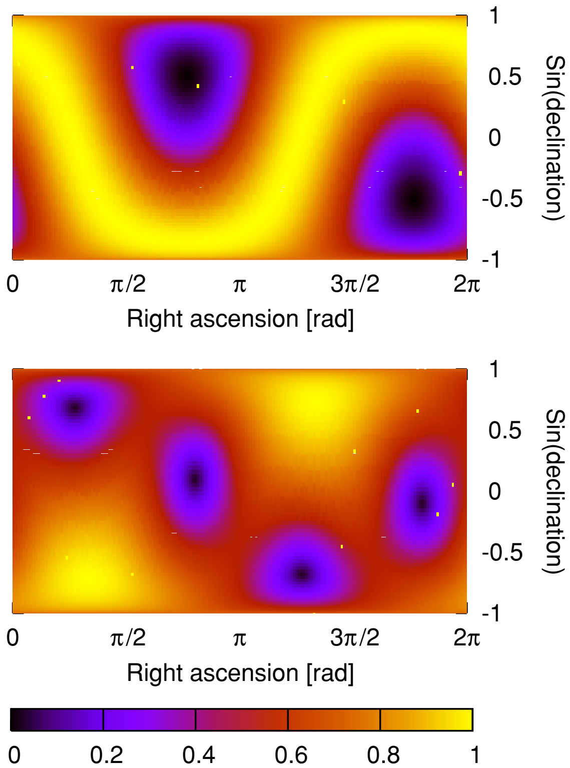

Figure 3. Top: antenna pattern magnitude of the AURIGA detector, function of the right ascension (ϕ) and declination (θ) angles on 23 September, 00:00:00 GMT. Bottom: antenna pattern magnitude for the LIGO-Hanford (LHO) detector, on the same date.

For linearly polarized signals, the upper portion of figure 4 shows the absolute value of this quantity, averaged over all possible polarizations. The bottom portion of figure 4 shows instead the average directional sensitivity of the AURIGA–LHO pair for circularly polarized signals, in which case the phase shift term can be neglected, the phase terms can be absorbed into a time shift $\Delta t = (\delta_1 - \delta_2)/4\pi f_0$ ($2\pi f_0$ is the time derivative of ψ [8]) and equation (5) can be simplified to

$$F_1 F_2 = A_1 A_2. \tag{6}$$

The network sky coverage, defined as detection efficiency as a function of the source location, depends on the data analysis method and on the sensitivity of each detector. In particular, since AURIGA is less sensitive than the LIGO interferometers, the AURIGA/LIGO-Hanford (LHO) and the AURIGA/LIGO-Livingston (LLO) pairs do not offer a significant improvement on the sky coverage of the LHO–LLO pair. Figure 5 shows the sky coverage of the three-fold configuration AURIGA–LHO–LLO assuming that each detector applies a threshold prior to a coincidence search (see section 5.1). In order to account for its lower sensitivity, the threshold for AURIGA is assumed to be three times larger than the one of a LIGO interferometer. For a signal amplitude ten times the LIGO threshold, more than half of the polarizations are covered for a large portion of the sky.

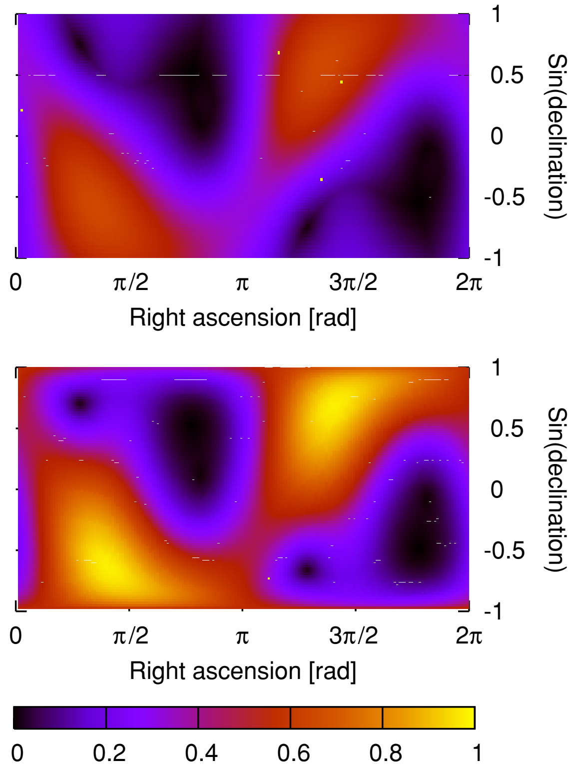

Figure 4. Top: polarization average of the product of the antenna patterns for AURIGA and LHO, function of the right ascension (ϕ) and declination (θ) angles on 23 September, 00:00:00 GMT. This is the sky coverage of the detector pair for linearly polarized signals. Bottom: polarization average of the product of the antenna patterns for AURIGA and LHO in the case of circularly polarized signals, on the same date.

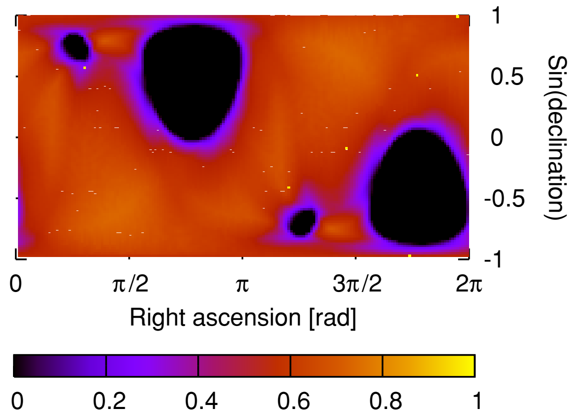

Figure 5. Sky coverage of the three-fold configuration AURIGA–LHO–LLO, to be interpreted as the detection efficiency averaged over polarizations, which are assumed to be uniformly distributed. The detection strategy is the time coincidence described in section 5.1. The AURIGA threshold is assumed to be a factor 3 larger than the LIGO threshold. The incoming signal in this calculation is 10 times above the LIGO threshold. Right ascension (ϕ) and declination (θ) angles are computed for 23 September, 00:00:00 GMT.

4. Scientific motivation for an AURIGA–LIGO joint burst analysis

Despite the fact that in a trigger-based analysis the sky coverage is not improved by the addition of the AURIGA bar detector to the LIGO network, there are several motivations to pursue this type of analysis.

Obvious advantages are the false alarm suppression and the improved ratio between false detections and detected events. Moreover, the addition of a detector increases the observation time during which three or four detectors were operating in coincidence. In the AU1/S3 coincidence period, there were 92 h of four-fold coincidence and an additional 175 h of three-fold coincidence, with two of the LIGO interferometers running in coincidence with the AURIGA resonant bar.

Even more important is the fact that a 4-detector network provides better confidence in a possible detection and the ability to completely characterize the properties of a detected signal. A complete solution of the 'inverse problem' consists of two coordinates for direction and two polarizations for amplitude. In the case of a network of three non-co-located detectors, such as LHO, LLO and AURIGA, we can get overabundant information on the source and completely characterize the properties of the associated wave.

5. General strategy for a trigger-based analysis

This section outlines the planned strategy for the AURIGA–LIGO burst analysis.

The first step consists of data quality assessments and veto implementation, separately performed by each collaboration prior to the data exchange. For AURIGA this means the application of both first level vetoes, established *a priori* by detector characterization, and second level vetoes, for periods of non-gaussianity or with degraded detection efficiency. In LIGO, a set of data quality flags is established by detector characterization investigations and diagnostic vetoes are implemented on the basis of coincidences between gravitational and auxiliary channels.

The next step is for the two collaborations to exchange burst candidate events found by their respective algorithms [9, 10, 12]. The standard quantities to be exchanged for each events are the arrival time, the band-limited calibrated amplitude A and their errors. In addition, it is important to also exchange the sensitivity of the detectors at all times. This quantity, referred to as A_T, is the minimum detectable amplitude, or the amplitude above which the event parameter estimation is trustworthy. Only events with amplitude exceeding A_T are to be exchanged.

A preliminary tuning of the analysis takes place on a 10% subset of the data set, referred to as the *playground*. The final analysis thresholds are fixed by using coincident events obtained in the whole data set after shifting the time axis of one or more detectors by unphysical delays, larger than the maximum light travel time between detectors but small enough to preserve stationarity. The analysis is frozen before looking at the real coincident events, as all decisions on the analysis are to be made while blind to the final results in order to avoid biases due to *a posteriori* choices, which could jeopardize the statistical interpretation of the results.

The fundamental idea for the network search is to compare the information from the different detectors through a conveniently chosen test statistic. In order to evaluate its significance, the measured value is compared to its background, off-source distribution, which is obtained from the introduction of several unphysical delays between the detectors. Given the measured test statistic and its estimated background distribution, it is possible to set a confidence interval, for instance, on the number of gravitational waves that crossed a minimum number of detectors within a given time period.

The interpretation of the final result requires assumptions on the source properties: location, polarization angle and waveform. In order to calibrate the results and their statistic, the detection efficiency is computed for selected signal classes and source distributions using Monte Carlo simulations. Alternatively, it is possible to optimize the search with some assumptions on the source characteristics.

In this context, we propose two alternative pipelines. The first is optimized for a target source direction and polarization, with the expectation that different angular combinations will be probed in order to map the sky. The second one makes no assumptions on source direction or polarization, except for an upper bound on the signal duration. In the hypothesis that both pipelines can be implemented, their overlap and the possibility to combine them into a single result can be tested, in a blind procedure, on the time-delayed background data [2].

5.1. Method 1: directional analysis

The first proposed approach is a trigger-based directional analysis that follows the main guidelines of the IGEC procedure [2], with three fundamental differences:

(i) the polarization angle of the wave cannot be neglected, as one could do with almost parallel and identical detectors;
(ii) the power spectral density of the detectors are significantly different;
(iii) the analysis is performed over a broader frequency band and the δ-matched filter cannot be used to estimate the amplitude of an event.

In the context of a directional analysis, the most delicate point is the definition of the events' amplitude. A few options are possible. In the IGEC analysis, which only includes bar detectors with similar narrow-band sensitivity and orientation, events are identified by matched filtering the whitened data with a δ-function template. The filter provides an optimal estimate of arrival time and calibrated amplitude. In the AURIGA–LIGO network, the situation is complicated by the fact that some of the detectors are broadband and more freedom in the choice of templates would be needed. In a template-based analysis, the event amplitude would first be estimated by the event trigger generator in the frequency range where each detector is sensitive (narrow band for the bar and broadband for the interferometers). For each template, this quantity can be scaled into a calibrated amplitude to be used in the network coincidence. Alternatively, a completely templateless search can be performed in the narrow band where all detectors have comparable sensitivity (850–950 Hz), although this would constitute a limitation for the LIGO interferometers, whose best sensitivity is at lower frequencies. A third possibility is to make general assumption on the shape of the waveform, such as smoothness or asymptotic spectral slope at high frequency, in order to use all out-of-band LIGO events and extrapolate the narrow-band component of the signal that is to be used in the network analysis.

The current plan is to adopt the templateless parameter estimation technique first introduced in the LIGO burst analysis [11], where the event time is estimated through a maximum likelihood fit and the band-limited event amplitude A_{meas} is defined as the square root of the excess power, in this case band-limited to 850–950 Hz.

The exchanged data (time and A_{meas} for each event and the minimum detectable amplitude A_T at all times) are fed into a network coincidence module that is optimized for a given direction (the Galactic Center is a good starting point, but the complete analysis would explore different directions and map the sky) and signal polarization. IGEC involved only co-aligned bar detectors, therefore the source polarization did not need to be taken into account. The key point is to apply a time-dependent antenna pattern correction for the chosen direction

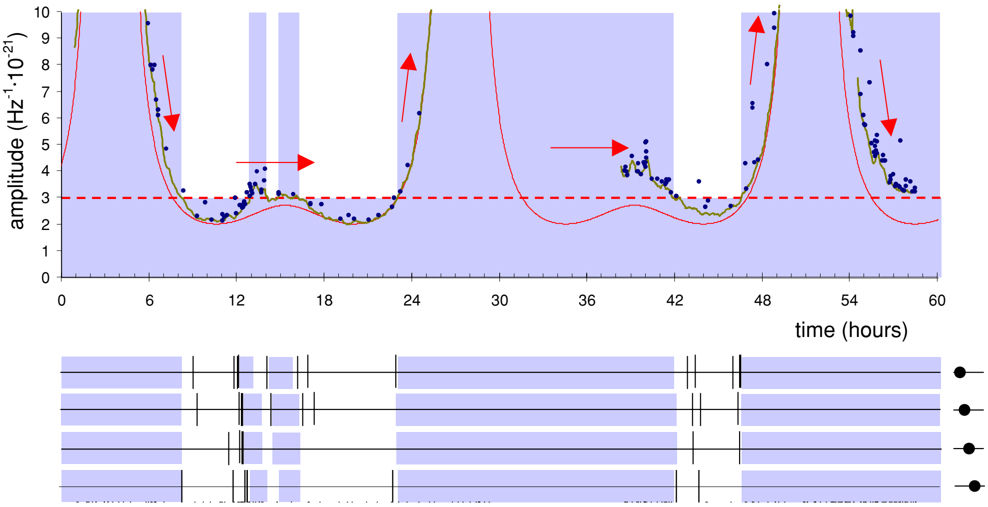

Figure 6. Trigger-based directional analysis. The top panel illustrates the proposed data selection mechanism for the directional analysis, using 60 h of AURIGA data. The variable on the vertical axis is the strain amplitude of a gravitational wave from the Galactic Center direction. In this example, the amplitude is the Fourier component of the strain at $\sim$900 Hz and, for the sake of simplicity, only the polarization component aligned with the detector is considered. Each dot represents a measured trigger, with its time as horizontal coordinate and $A_{\rm source}$ as vertical coordinate. $A_{\rm source} = A_{\rm meas}/F$ is the estimated event amplitude at the Galactic Center, related to the measured amplitude $A_{\rm meas}$ through the time-dependent antenna pattern F. The angular sensitivity modulation $1/F$ is proportional to the solid smooth line. The solid jagged line is A_T/F, the minimum detectable amplitude for the Galactic Center direction, A_T being the detector's instantaneous sensitivity. The horizontal dashed line represents a fixed absolute threshold on $A_{\rm source}$. The data selection consists of discarding all events with $A_{\rm source}$ below this threshold and all the observation time in which the minimum detectable amplitude is above this threshold (vertical shadows). The first row in the bottom panel represents the resulting 'on-source' time series, where the vertical lines correspond to events with $A_{\rm source}$ above threshold and the white bands represent the time intervals with detector sensitivity below threshold (the effective live time). This time series is put in coincidence with similar ones from other detectors, obtained with the same common $A_{\rm source}$ threshold. The remaining rows in the bottom panel represent background, 'off-source' time series. These are obtained with a shift of the local time coordinate by set amounts. In the top panel, this would correspond to sliding all the dots and the detector threshold along the directions indicated by the arrows. Off-source time series with different time shifts from different detectors yield the accidental rate for the coincidence analysis.

and polarization to $A_{\rm meas}$ and derive the corresponding $A_{\rm source}$, a quantity that can be directly compared in all detectors. In order to enhance the detection confidence, the live time is to be constrained to periods when A_T, scaled by the antenna pattern factor, is comparable between detectors, as exemplified in figure 6 and its caption. Even with no antenna pattern correction, this data selection step would be necessary to compensate for fluctuations of the detector sensitivity.

The final test statistic is the number of coincidences between a minimum number of detectors (for instance, three out of four) with $A_{\rm source}$ above a given threshold in different detectors.

This procedure would be repeated on a set of directions and polarizations, in order to cover the whole sky.

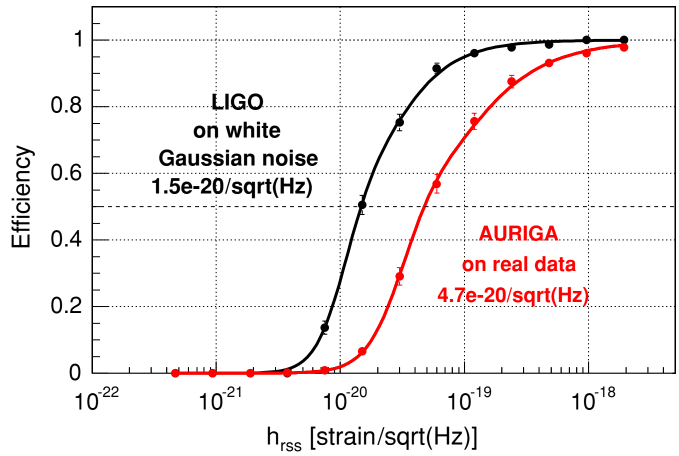

Figure 7. Expected performance of method 2 for sine-Gaussian with central frequency $f_0 =$ 900 Hz and $Q = 9$.

5.2. Method 2: 'eyes wide open'

The alternative analysis pipeline follows the all-sky 'eyes wide open' approach used in the LIGO burst analysis [3], where no assumptions are made on the event waveform, polarization or direction.

The plan is to implement it as a coherent search within the LIGO interferometers triggered by the AURIGA events, where AURIGA provides a list of events produced with the δ-matched filter and LIGO performs a search around those times with CorrPower [12], a code based on cross-correlation for the detection of excesses of coherent power between the three LIGO interferometers.

CorrPower estimates the event's coherent power within a factor of 2, which is not accurate enough for a directional analysis. This method is designed as an 'all-sky' search, where no assumptions are made on the relative amplitude of the LIGO and the AURIGA events.

The detection efficiency is determined through Monte Carlo simulations, as is typically done in the LIGO burst search [3], under the assumption of either an isotropic or a galactic-plane population model and random source polarization. The simulation scheme is the one already implemented in LIGO, where a single engine produces data frames with the waveforms as they would appear in all detectors at given time stamps. The engine accounts for the source position, polarization and orientation. In order to reconstruct detection efficiency curves, the waveforms can be scaled by several multiplicative factors and added to the detector noise before being analysed by the full pipeline.

Figure 7 shows the expected performance in this type of analysis, where the simulated waveform is a sine-Gaussian with central frequency $f_0 = 900$ Hz and $Q = 9$. The sources are assumed to be uniformly distributed on a sphere around earth, with random polarization. The LIGO curve has been produced using white Gaussian noise, matching the median 800–1000 Hz band-limited rms during the AURIGA–LIGO coincidence run (see figure 1); CorrPower was run with a threshold $\Gamma_0 = 4$ (see [12] for explanations of the meaning of this threshold), which is smaller than the typical threshold used in the LIGO-only analysis for the S3 science run, but can realistically be implemented in a four-fold coincidence with AURIGA. The AURIGA efficiency curve uses the Monte Carlo average detection efficiency obtained with the δ-filter on sine-Gaussian waveforms and actual detector noise, prior to the implementation of vetoes. The threshold on the AURIGA triggers is SNR > 4. The implementation on actual data will allow setting more realistic thresholds, based on the false alarm rate allowed in the analysis. The network efficiency is approximately equal to the product of the two curves; the 50% detection efficiency points are roughly a factor 3 worse for AURIGA than for the LIGO detectors, consistent with expectations. Since the LIGO curve was obtained on ideal white Gaussian noise, some performance degradation is expected on real data.

This second method is in a more advanced stage of development, and it is the one currently being implemented.

6. Conclusions

A working group has been formed to perform a joint burst search in LIGO and AURIGA, with the goal to develop and apply to real data methodologies for joint searches between bar detectors and interferometers.

The team is addressing a time coincidence, triggered-based search on data acquired during a 2-week period, between 24 December 2003 and 9 January 2004, when the upgraded AURIGA and LIGO were simultaneously functioning. Two strategies have been outlined: an optimized directional analysis to be applied to a set of directions and an all-sky search that does not make assumption on the source position. The data exchange is under way, and priority is being given to the all-sky analysis method.

Acknowledgments

This work was supported by the US National Science Foundation under Cooperative Agreement No PHY-0107417 and by the Istituto Nazionale di Fisica Nucleare (INFN). Baggio acknowledges the hospitality of ICRR.

References

[1] LIGO Documents M040010-00-M and M040191-00-M http://antares.ligo.caltech.edu/dcc/
[2] IGEC Collaboration 2003 Methods and results of the IGEC search for burst gravitational waves in the years 1997–2000 *Phys. Rev.* D **68** 022001 (*Preprint* astro-ph/0302482)
[3] LIGO Scientific Collaboration 2004 *Phys. Rev.* D **69** 102001
[4] Flanagan E E and Hughes S A 1998 *Phys. Rev.* D **57** 4535
[5] Baker J, Campanelli M, Lousto C O and Takahashi R 2002 Modeling gravitational radiation from coalescing binary black holes *Phys. Rev.* D **65** 124012 (*Preprint* astro-ph/0202469)
[6] Zendri J P *et al* 2000 Status report of the gravitational wave detector AURIGA *Gravitational Waves: Proc. 'Third Edoardo Amaldi Conference' (Caltech, 1999)* ed S Meshkov (AIP Conference Proceedings, New York) pp 421–2
[7] http://www.auriga.lnl.infn.it
[8] Gursel Y and Tinto M 1989 *Phys. Rev.* D **40** 3889
[9] Ortolan A *et al* 1998 Data analysis for the resonant gravitational wave detector AURIGA: optimal filtering, Chi-square test, event timing and reconstruction *Proc. 'Second Edoardo Amaldi Conference on Gravitational Wave Experiments' (CERN, Switzerland, 1997)* ed E Coccia, G Veneziano and G Pizzella (Singapore: World Scientific) p 204
[10] Klimenko S and Mitselmakher G 2004 *Class. Quantum Grav.* **21** S1819–30
[11] Sylvestre J *LIGO/LSC Algorithm Library* available at http://www.lsc-group.phys.uwm.edu/lal/ **See endnote 1**
[12] Cadonati L and Márka Sz CorrPower: a cross-correlation-based algorithm for triggered and untriggered gravitational burst searches (these proceedings) **See endnote 2**

Endnotes

(1) Author: Please provide year in reference [11].
(2) IOPP: Please update reference [12].
(3) Author: Please be aware that the colour figures in this article will only appear in colour in the Web version. If you require colour in the printed journal and have not previously arranged it, please contact the Production Editor now.